Cape Peninsula
University of Technology

DESIGN AND SIMULATION OF A RESIDENTIAL ROOFTOP PV SYSTEM IN KIRSTENHOF, CAPE TOWN

by

Gift Rethabile Mthombeni

241297095

Industrial Design Project 3 submitted in fulfilment of the requirements for the degree

Bachelor of Engineering Technology in Electrical Engineering

in the Faculty of Engineering and the Built Environment

at the Cape Peninsula University of Technology

Bellville campus

Date submitted (October 2025)

DECLARATION

I, Gift Rethabile Mthombeni, declare that the contents of this dissertation/thesis represent my own unaided work, and that the dissertation/thesis has not previously been submitted for academic examination towards any qualification. Furthermore, it represents my own opinions and not necessarily those of the Cape Peninsula University of Technology.

Signed **Date**

SUMMARY

The growing demand for reliable, secure, and sustainable energy has accelerated the adoption of renewable-based distributed generation, particularly residential rooftop photovoltaic (PV) systems. This study presents the design and simulation of a grid-tied residential PV system incorporating a PV array, hybrid inverter, and battery energy storage system (BESS). Using MATLAB Simulink, the system's technical performance was analysed under Cape Town's climatic conditions, while the System Advisor Model (SAM) was employed to assess its financial feasibility. The research focused on identifying performance limitations in the existing installation and developing an optimized configuration to enhance efficiency, reliability, and cost-effectiveness. The findings demonstrated that system optimization significantly improved inverter utilization, energy yield, and economic viability, confirming the potential of residential PV-BESS systems to reduce grid dependency and support sustainable energy adoption in South Africa.

Keywords: renewable-based energy sources, distributed generation, residential rooftop PV systems, MATLAB Simulink, System Advisor Model (SAM).

TABLE OF CONTENTS

LIST OF FIGURES

LIST OF TABLES

APPENDIX/APPENDICES

Appendix A: MATLAB setup

GLOSSARY

Abbreviation	Full Term
AC	Alternating Current
Ah	Ampere-hour
BESS	Battery Energy Storage System
CAPEX	Capital Expenditure
DC	Direct Current
DOD	Depth of Discharge
GHI	Global Horizontal Irradiance
I–V	Current–Voltage
IEC	International Electrotechnical Commission
INV	Inverter
kWh	Kilowatt-hour
kW/m²	Kilowatt per Square Metre
LCOE	Levelized Cost of Energy
Li-ion	Lithium-ion
MPPT	Maximum Power Point Tracking
NPV	Net Present Value
OPEX	Operational Expenditure
P–V	Power–Voltage
PV	Photovoltaic
ROI	Return on Investment
SAM	System Advisor Model
SOC	State of Charge
SoH	State of Health
TOU	Time-of-Use
V	Volt
W	Watt
Wh/kg	Watt-hour per Kilogram
η	Efficiency

1. Introduction:

1.1. Background and Context

South Africa continues to face serious energy challenges, with frequent load-shedding and rising electricity costs caused by Eskom's ageing infrastructure and limited generation capacity. In Cape Town, these challenges have encouraged many homeowners to explore rooftop solar photovoltaic (PV) systems as a reliable and sustainable alternative for meeting household electricity needs.

This project focuses on the design and simulation of a residential rooftop PV system with battery energy storage, located in Kirstenhof, Cape Town. The main goal is to improve energy reliability, reduce grid dependence, and assess the technical and financial feasibility of such systems under local operating conditions. The system includes a PV array, hybrid inverter, and battery storage unit, configured to optimize energy generation, storage, and utilization. The project was initiated in response to growing interest in small-scale embedded generation within Cape Town, where households seek solutions that can provide backup power during load-shedding and reduce monthly electricity expenses. By simulating the system in MATLAB Simulink and conducting a financial evaluation in the System Advisor Model (SAM), this study provides practical insights into how residential PV systems can be optimized for better performance and cost-effectiveness.

Ultimately, this work contributes to improving energy resilience at the household level and supports the City of Cape Town's broader goal of promoting decentralized renewable energy adoption in urban areas like Kirstenhof.

1.2. Problem Statement

The integration of residential photovoltaic (PV) systems with battery energy storage often faces challenges related to poor system sizing, inefficient control strategies, and unstable power flow. These issues result in underutilized inverters and batteries, inconsistent energy supply, and reduced overall system efficiency. Additionally, high installation costs and uncertain financial returns further limit adoption and long-term sustainability. This study addresses these challenges by investigating the optimal design and simulation of a grid-tied rooftop PV system with battery storage to improve energy management, enhance performance under varying operating conditions, and evaluate its technical and financial feasibility.

1.3. Objectives and Scope Definition

This study aimed to investigate and improve the performance of a residential rooftop photovoltaic (PV) system integrated with battery energy storage. The specific objectives were to:

1. **Diagnose and analyse** the technical causes of the system's underperformance through modelling and simulation in MATLAB/Simulink, focusing on inverter utilization, PV generation efficiency, and battery charging behaviour.
2. **Develop and evaluate** an optimized system configuration (upgraded PV array) to improve energy flow, enhance storage utilization, and ensure stable operation under Cape Town's climatic conditions.
3. **Assess the financial feasibility** of both the base and optimized system configurations using the System Advisor Model (SAM), determining the impacts on LCOE, NPV, payback period, and overall economic viability.
4. **Compare and interpret** the technical and financial outcomes of both cases to recommend an optimal configuration that balances performance, reliability, and cost-effectiveness for residential applications

2. Understanding the Design Scope

2.1 Identification of Project Objectives

The project aimed to model, simulate, and assess the performance of a residential rooftop photovoltaic (PV) system integrated with a battery energy storage system (BESS) and inverter under Cape Town's operating conditions. The focus was on identifying how energy generation, storage, and utilization could be optimized to improve reliability during load-shedding and reduce grid dependency. The scope was intentionally limited to surface-level problem solving, addressing only the conceptual and analytical aspects of system performance rather than full-scale engineering implementation. This study does not constitute professional design advice but an academic investigation intended to provide insight into system feasibility and operation.

2.2 Analysis of Project Objectives

The objectives of this project were analysed to ensure alignment with the overall goal of improving the technical and financial performance of the residential photovoltaic (PV) system integrated with battery energy storage. Each objective was structured to address specific system challenges under Cape Town's load-shedding conditions.

- The first objective focused on diagnosing and analysing the system's underperformance through MATLAB/Simulink modelling. This involved assessing inverter utilisation, PV generation efficiency, and battery behaviour to identify operational inefficiencies and areas for improvement.
- The second objective centred on developing and evaluating an optimised PV system configuration. Simulations tested different design scenarios to enhance energy flow, maximise inverter matching, and ensure reliable operation during periods of variable solar irradiance.
- The third objective examined the financial feasibility of both the base and upgraded systems using the System Advisor Model (SAM). Key financial indicators such as the Levelized Cost of Energy (LCOE), Net Present Value (NPV), and payback period were evaluated to determine cost-effectiveness.
- The final objective compared and interpreted the results of both configurations to identify the optimal balance between technical performance and economic viability. This comparison provided insights into the trade-offs between cost, reliability, and energy yield.

Overall, the analysis confirmed that the objectives were clear, measurable, and achievable within the project scope, effectively guiding the study toward enhancing the performance and feasibility of residential PV–BESS systems in Cape Town.

2.3 Criteria Formulation for Design Solution

The criteria for evaluating the success of this study were based on the extent to which the project's objectives and research questions were effectively addressed. Success was determined by the ability of the system model to demonstrate stable and realistic energy flow between the PV array, inverter, and battery under the simulated conditions.

The design was considered successful if the analysis and simulations provided meaningful insight into the system's technical and financial feasibility, particularly in relation to energy efficiency, storage performance, and grid dependency reduction. Since the study was conducted within an academic framework, the evaluation focused on conceptual accuracy and analytical outcomes rather than full-scale implementation. In this context, the successful resolution of the research problems served as the key performance indicator for the overall study

3. Broadly Defined Problem Solving: Considering Solutions

3.1 Problem Definition and Analysis

Research questions:

Technical Questions

1. How can the integration of the PV array, hybrid inverter, and battery energy storage system (BESS) be optimized to improve energy flow and overall system efficiency?
2. How does the system perform under varying environmental conditions such as solar irradiance, temperature, and load demand?
3. What control and management strategies can be implemented to enhance battery utilization, minimize degradation, and ensure stable system operation?

Financial Questions

1. What is the economic viability of the residential rooftop PV-BESS system in terms of Levelized Cost of Energy (LCOE), Net Present Value (NPV), and payback period?
2. How does the optimized PV configuration impact total investment cost, operational savings, and long-term financial performance?
3. To what extent can system optimization reduce dependency on the national grid and improve the return on investment (ROI)?

3.2 Development of Design Approach

Research Methodology

This study adopted an applied research approach aimed at diagnosing and resolving performance deficiencies in an existing solar photovoltaic (PV) system. The methodology was structured to identify the root causes of underperformance, design corrective solutions through simulation-based analysis, and evaluate the technical and financial feasibility of the proposed interventions. The research process followed a systematic flow from problem identification to data collection**,** simulation analysis, and recommendation formulation**,** ensuring both scientific rigour and practical applicability.

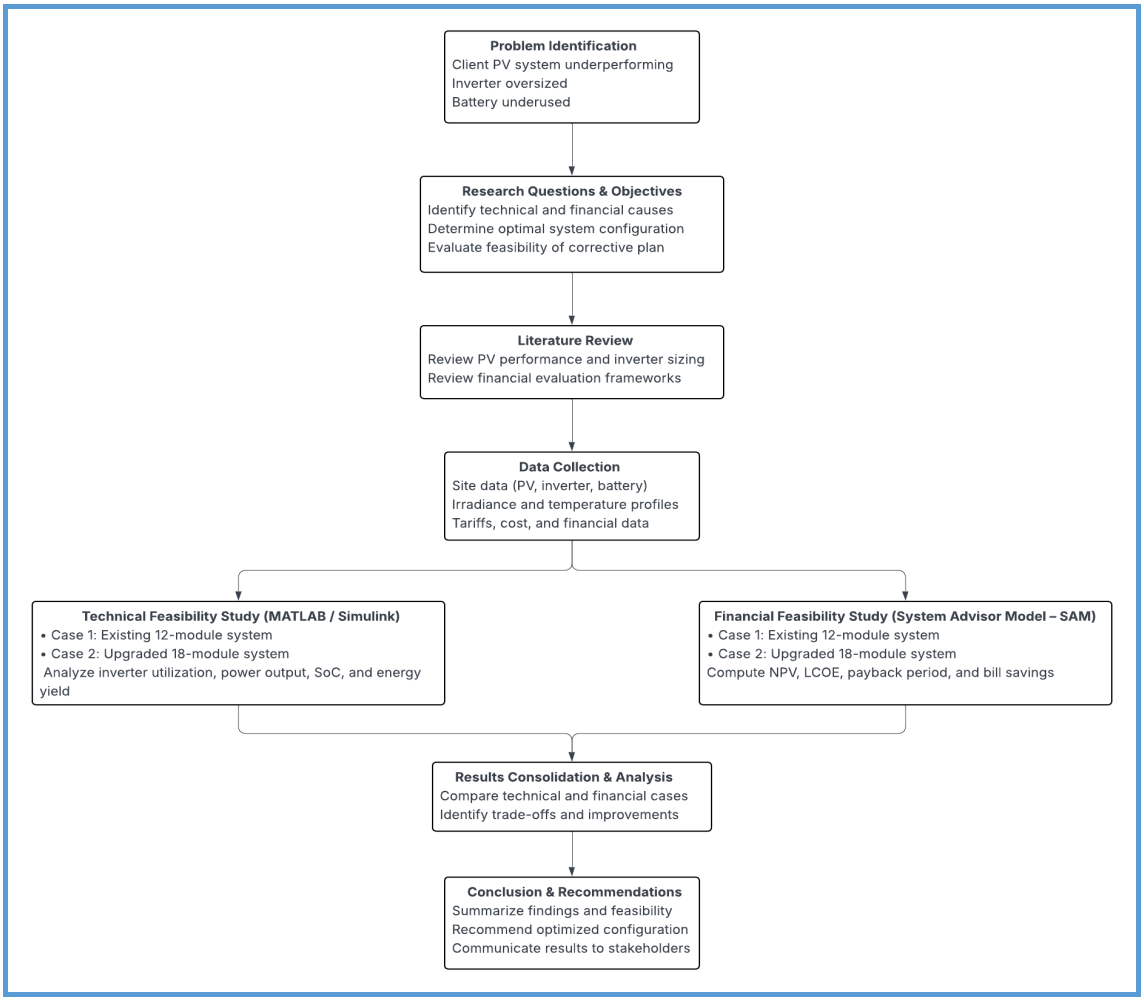

Figure 1: Flow chart showing the methodology approach

The research design was primarily diagnostic and experimental, involving both qualitative assessments (problem identification and stakeholder interviews) and quantitative analysis (simulation-based modelling).

4. Implementing Design Strategy

4.1 Solution Execution

4.1.1 Literature review

PV SYSTEM:

The growing global shift toward renewable energy has significantly increased the integration of solar power systems. Solar energy is primarily harnessed through photovoltaic (PV) generation, where solar cells connected in series or parallel within a module convert sunlight into electricity via the photovoltaic effect (Ma et al. 2019), (Patel, Gupta and Bohre, 2016). Owing to advances in PV technology, these systems have become simpler to install and operate, driving widespread adoption by building owners seeking to utilize clean, renewable energy and reduce dependence on grid electricity (Brano et al. 2010), (Osmani et al. 2020).

The performance of PV modules depends mainly on solar irradiance and conversion efficiency, which are influenced by factors such as weather conditions, panel orientation, and electrical loading (Brano et al. 2010). However, power ratings provided by manufacturers are often based on standardized test conditions—namely, the Standard Test Conditions (STC) and the Nominal Operating Cell Temperature (NOCT)—which may not accurately represent real-world performance under varying environmental conditions (Ma et al. 2019).

PV Technology

Chemical composition

A photovoltaic (PV) cell consists of two semiconductor layers—p-type and n-type—forming a p–n junction that enables the conversion of sunlight into electricity (Patel, Gupta and Bohre, 2016). Silicon is the primary semiconductor material, where boron doping creates the p-type layer and phosphorus doping forms the n-type layer. When exposed to light, photons excite electrons, causing them to move across the junction through diffusion, leaving behind ions that generate an internal electric field. This field drives electron flow, producing current directly proportional to the incident irradiance (Sproul 2003).

Crystal structure

Various PV technologies exist, including crystalline silicon, thin-film, amorphous silicon, perovskite photovoltaic (PPV), and bifacial solar cells, with crystalline silicon (C-Si) being the most widely used (Sproul 2003). C-Si cells are categorized into monocrystalline and polycrystalline types, fabricated using the Czochralski and ingot casting methods, respectively (Dobrzański *et al.* 2013). The Czochralski process yields high-purity single-crystal structures, while ingot casting produces multiple crystal fragments, giving polycrystalline cells their distinctive bluish hue (Sproul 2003) , (Jiang et al. 2020). Studies confirm that monocrystalline cells generally achieve higher efficiencies and superior performance than their polycrystalline counterparts, with recorded efficiencies of 9.22% and 7.94%, respectively (Jiang et al. 2020), (Hidayanti 2020).

Environmental conditions

Temperature

Only about 15–20% of incident solar irradiation is converted into electricity, while the remainder is dissipated as heat within the PV module (Rahman, Hasanuzzaman & Rahim 2015). This heat accumulation raises the operating temperature of the panels (Amelia *et al.* 2016), which is a critical factor affecting cell efficiency (Rao *et al.* 2024). As reported in (Brano *et al.* 2010), PV efficiency decreases noticeably with rising temperature, typically by 0.40–0.50% for every 1°C increase under standard operating conditions (Amelia *et al.* 2016), (Natarajan *et al.* 2011). The study in (Amelia *et al.* 2016) further demonstrated that while current may slightly increase, the output voltage—and consequently power—declines as temperature rises. Experimental results from (Kumar, Balasubramanian & Maheswari 2019) showed that PV efficiency dropped from 12.51% to 11.09% as temperature increased from 38.55°C to 44.15°C, accompanied by reduced solar irradiance (754 W/m² to 633 W/m²). This temperature-dependent degradation occurs across both monocrystalline and polycrystalline silicon technologies (Rao *et al.* 2024).

Solar irradiance

Solar irradiance, measured in watts per square meter (W/m²), represents the amount of solar power incident on a given surface area (Wikipedia 2025a). It significantly influences both the temperature and electrical performance of solar cells (Rahman, Hasanuzzaman & Rahim 2015). Under typical conditions, a solar cell's temperature can rise by approximately 4.93°C for every 100 W/m² increase in irradiance (Rahman, Hasanuzzaman & Rahim 2015). As observed in (Amelia *et al.* 2016), irradiance and ambient temperature tend to increase simultaneously throughout the day, affecting cell behaviour and output. Increased irradiance enhances both open-circuit voltage and current, thereby improving overall power generation (Amelia *et al.* 2016), (Koondhar *et al.* 2022). According to (Rahman,

Hasanuzzaman & Rahim 2015), output power may increase by about 4.35 W with cooling and 2.94 W without cooling for every 100 W/m² rise in solar irradiance."

Humidity

"Humidity is the concentration of water vapour present in the air" (Wikipedia 2025b). Humidity can compromise PV module's performance and reduce the output power from the solar panels by up to 15-30% (Panjwani & Narejo 2014). (Rahman, Hasanuzzaman & Rahim 2015) conducted an investigation whereby the irradiation level was kept at 800W/m2 to measure the output power at varying relative humidity values and the power output were documented as follows: 25.31 W at 40% humidity, 23.76 W at 50% humidity, and 22.15 W at 60% humidity, and a distinct decrease in power with an increase in humidity is clearly observed. (Kazem & Chaichan 2015) Presented a more elaborate and nuanced examination, stating that:

- Relative humidity is typically higher during night hours
- "The air water vapour contents affect the solar irradiance level and reduce the solar intensity by scattering the radiation".

And subsequently concluding that relative humidity diminish a solar cell current, voltage, power, and efficiency.

INVERTER SYSTEM:

Grid-connected non-dispatchable energy sources, such as PV and BESS systems, require a power conversion system to transform DC output into AC, typically achieved through an inverter (Franco *et al.* 2021). Inverters play a vital role in maintaining grid stability and ensuring reliable operation, especially in systems comprising multiple PV arrays. Their main function is to continuously track the Maximum Power Point (MPP) under varying irradiation and environmental conditions. However, excessive temperature increases can impair inverter performance and lead to hotspot formation (Kolantla et al. 2020). A key design consideration involves selecting the integration architecture—either DC-coupled or AC-coupled—which determines the type of inverter used (He, Yang & Vinnikov 2020). Modern inverters have evolved to provide additional grid-support functions, including spinning reserves, voltage regulation, frequency response, ramp-rate control, and variability smoothing (Franco *et al.* 2021)

Inverter Technology

Inverter Type and Topologies:

Two main types of inverters are commonly used in PV systems: single-phase and three-phase. A single-phase inverter converts the DC power generated by photovoltaic modules into AC power at 220–230 V, typically using a three-terminal wiring configuration. In contrast, a three-phase inverter delivers higher power by producing three AC outputs phase-shifted by 120°, with a standard output voltage of 380–400 V and a five-terminal configuration (China Gode 2025).

In terms of topology, three principal inverter configurations are widely applied. The central inverter is used for large-scale systems ranging from several hundred kilowatts to a few megawatts. Multiple PV strings are connected in parallel through diodes, isolators, and fuses to prevent reverse current flow and allow string isolation. Central inverters perform global Maximum Power Point Tracking (MPPT) and manage complex control functions such as islanding detection (Kolantla *et al.* 2020). The string inverter topology connects multiple PV modules in series, forming strings that typically operate between 150–450 V and up to 2–3 kW. These inverters often employ an H-bridge or full-bridge configuration (Kolantla *et al.* 2020). Lastly, micro-inverters are attached to individual PV modules, allowing independent MPPT, improved performance under partial shading or mismatch, and enhanced overall system reliability (Kolantla *et al.* 2020).

Switching Techniques:

Inverters convert DC power to AC by the controlled switching of semiconductor devices such as IGBTs, MOSFETs, or SiC transistors, which are turned on and off in a defined sequence to

synthesize an AC waveform from the DC input. The two primary switching techniques used are Pulse-Width Modulation (PWM) and Sinusoidal Pulse-Width Modulation (SPWM).

In a PWM inverter, three single-phase inverters operate with sinusoidal control voltages phase-shifted by 120°, where frequency regulation is achieved by varying the control signal frequency. PWM provides several advantages, including a wide linear modulation range, reduced switching losses, lower total harmonic distortion (THD), and simple implementation with minimal computational requirements (Kolantla *et al.* 2020).

SPWM, on the other hand, produces the AC output by modulating pulse widths based on the comparison between a sinusoidal reference and a high-frequency carrier wave, typically triangular or saw tooth in shape. The modulation process adjusts pulse width according to the amplitude and frequency of the reference signal, allowing precise control over the inverter's output voltage and frequency (Kumar, Michael, John & Kumar 2010).

Environmental & Operational Conditions

Inverters, like all electronic systems, experience gradual degradation over time due to both operational and environmental factors (Jarosz-Kozyro & Baranowski 2025). Conditions such as temperature fluctuations, humidity, dust, and precipitation can continuously affect their efficiency and reliability. Since inverters perform critical functions like Maximum Power Point Tracking (MPPT) and DC-to-AC conversion, maintaining their performance is essential to ensure overall system stability and dependability (Idbouhouch et al. 2024).

A study by (Kshatri, Dhillon & Mishra 2021) examined the effects of solar irradiance and ambient temperature on inverter reliability across different geographical regions. Using real-time data from India and Denmark, the results revealed that inverter lifetimes are significantly shorter in hot climates compared to cooler ones, demonstrating the strong environmental influence on component durability.

Performance issues can also arise under specific operating conditions. For example, inverter clipping occurs when systems with high DC loading ratios are forced to limit power output under strong sunlight to avoid exceeding rated input capacity, leading to short-term efficiency losses (Anderson et al. 2022). Likewise, partial shading has been shown to disrupt inverter operation by causing shifts in the Global Maximum Power Point (GMPP). As reported in (Sezgin-Ugranlı 2025), this effect—largely determined by bypass diode configuration—results in voltage and power fluctuations at the inverter input, making system performance highly sensitive to irradiance variations and inverter design.

BATTERY ENERGY STORAGE SYSTEM (BESS)

The growing shift toward renewable energy sources such as wind, hydrogen, and solar power has introduced new complexities within modern distribution networks. These sources, often referred to as inverter-based generators, are inherently intermittent, with power output fluctuating according to environmental conditions. As a result, energy storage systems (ESS) have become essential to ensure grid stability and reliability (May, Davidson & Monahov 2018). Energy storage provides an alternative to traditional network reinforcements by storing surplus power and supplying it when needed to enhance system efficiency (Stecca et al. 2020), (Kwon et al. 2018). ESS technologies can generally be classified into five categories: thermal, mechanical, chemical, electrical, and electrochemical (Hannan et al. 2021).

Among these, Battery Energy Storage Systems (BESS)**—**a form of electrochemical storage—are the most widely adopted. In large-scale applications such as microgrids, BESS can provide synthetic inertia, frequency regulation, and power quality improvement (Stecca et al. 2020), (Hannan et al. 2021). In the context of residential photovoltaic (PV) systems, relevant to this study, BESS enables backup power during load shedding, load shifting, and enhanced energy autonomy—defined as "the time during which the load can be met with the battery alone, without any solar inputs" (PVsyst 2025).

Battery Technology

Chemical Composition:

There are various battery technologies available on the market, all suited for different applications, these include but not limited to lead acid, sodium-sulphur, Sodium-Nickel chloride, redox-flow and lithium-ion. The most widely used and commercially available technologies types are lithium-ion and lead-acid, their performance is shown in the figure below.

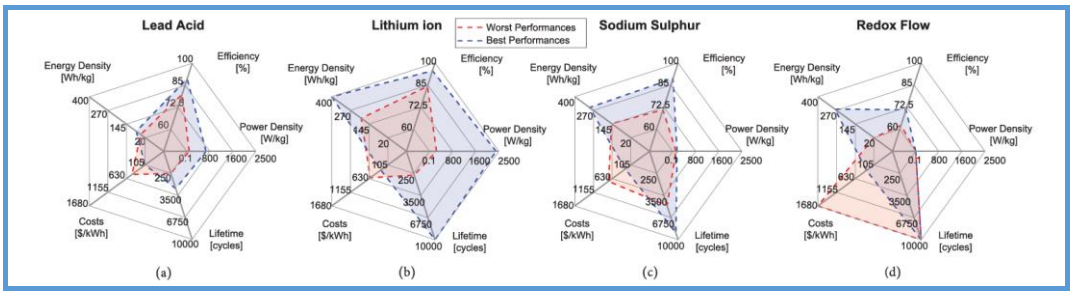

Figure 2: Performance comparison of Lead-Acid, Lithium-Ion, Sodium-Sulphur, and Redox Flow batteries across key metrics: energy density, power density, efficiency, cost, and lifetime**.**

Lead-acid batteries were the first rechargeable batteries, constituting several cells each of which consists of lead plates immersed in an electrolyte of dilute sulphuric acid (Electrical Academia 2025). Lead-acid battery technology has become well established in a sense that the manufacturing processes and supply chains have become highly optimized, and thus offering several advantages such as being relatively available and affordable but still limited by their lower volumetric energy density and adverse environmental impact. Lithium-ion (Li-ion) batteries retain electrical energy "in positive electrode materials made of lithium compounds capable of reversible intercalation of Li-ions and negative electrode materials made of carbon or graphite that can accommodate Li in the solid state" (May, Davidson & Monahov 2018). Lithium-ion ion offer advantages such as a relatively high volumetric energy density and low response latency but still limited by high capital costs and safety/handling concerns (Hannan *et al.* 2021).

Technology	Efficiency (%)	Cycles	Energy density(Wh/kg)
Lead-acid	75-90	300-3000	20-30
Lithium-ion	80-90	3000	90-190

Table 1: Comparison of Lead-acid and Lithium-ion battery performance metrics.

Over the past decade, Lithium-ion batteries have replaced Lead-acid batteries as the technology of choice, an as illustrated in the table above, it boasts impressive performance metrics give insights as to why it is the dominating technology.

Charge-Discharge Characteristics:

In choosing a battery energy storage system for any use case, there are a couple of characteristics that need to be taken into account this includes the capacity, battery life, efficiency, charge-discharge cycles, C-rate and depth of discharge (DoD). The paramount characteristic in this regard is the battery life. There is a direct correlation between the battery life and depth of discharge. Battery depth of discharge refers to the percentage of the total amount of energy stored in a battery that can be depleted without being detrimental to the batter (Rekioua 2023).

Performance

Temperature Effects:

Temperature has consistently posed a significant challenge and barrier to progress in battery technology advancements. High temperature, more specifically, efficiency, performance and safety of batteries, including but not limited to Lithium-ion batteries (Shen *et al.* 2022). (Zhang *et al.* 2021) Documents in his journal that, at elevated temperatures (>70), the degradation rate of battery capacity

can increase threefold, this is supported by literature as found in (Shen *et al.* 2022), whereby it is reported that:

- Battery capacity can decline by 38.9% during the first two charge/discharge cycles at 100°C
- Under elevated temperature conditions, the battery exhibited a pronounced reduction in voltage and capacity, accompanied by a substantial rise in impedance

In the context of this study, it is more especially important to consider the correlation between the state of charge (SoC) and Temperature. Reference can be made to (Taniguchi *et al.* 2019) who details out that the state of charge (SOC) is a critical factor affecting battery safety during high-temperature exposure. "The higher the SOC is, the worse the thermal stability is."

Charge/Discharge Rates:

Fast charging

Just like in electric vehicles (EV's), it is generally desirable for PV system batteries to have fast charging, however, research has proven that this can have adverse effects on the battery. In a review relating to challenges and issues facing ultrafast-charging lithium-ion batteries, (Aghili Mehrizi *et al.* 2025) points out that quick charging might create difficulties ranging from Lithium-ion components and charging methods to safety issues. High-rate charging is associated with various challenges, including mechanical damage, lithium dendrite formation, electrolyte instability, heat buildup, and thermal runaway, which impact battery safety and durability.

4.1.2 Data

Primary data were collected from the client's installed system, including PV module ratings, inverter capacity, battery specifications, and performance logs. These were complemented by secondary data from manufacturer datasheets, SAM databases, and relevant literature. Collected data were processed and used as input parameters in both the technical and financial simulation models. Quantitative results were analysed using comparative and descriptive analysis techniques to evaluate system performance across different scenario in this section comprehensive presentation of all pertinent data and information specific to the PV system is provided.

PV Specifications

Figure 3: Image showing the PV array on site

Specification	Value
Maximum Power	540 W
Maximum Power Voltage	40.7 A
Maximum Power Current	13.27 A
Open-Circuit Voltage	49.42 V
Short-Circuit Current	13.85 A
Module efficiency	20.90%

Table 2: Specifications for the PV module installed on-site

Inverter Specifications

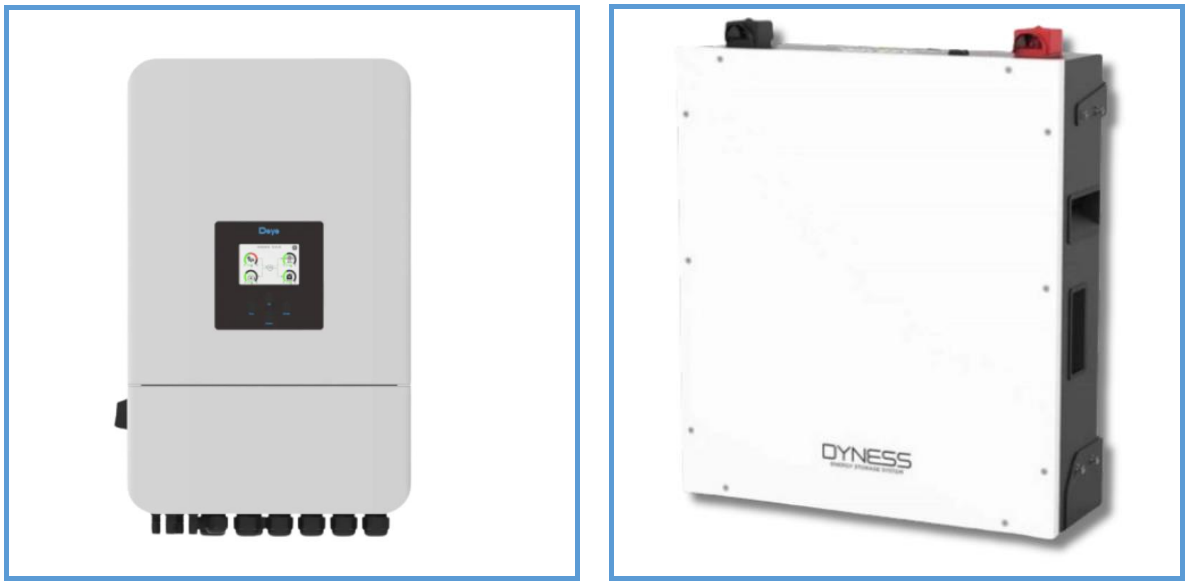

Figure 4: Deye hybrid inverter (left) and Dyness lithium-ion battery (right) used in the simulated PV-BESS configuration

Specification	Value
Brand	Deye
kW Size	8kW
Volt Size	48V
System Type	Hybrid
Maximum PV Array Power	10400W
Max Parallel Units	16

Table 3: Technical specifications of the Deye hybrid inverter used in the simulated PV–BESS configuration, showing power rating, voltage level, system type, and parallel operation capacity.

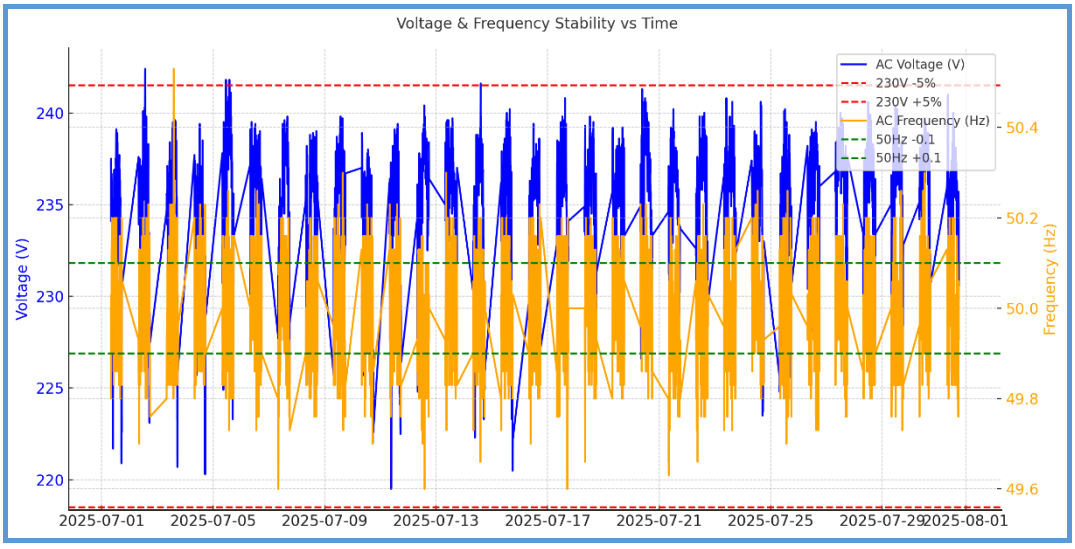

Figure 5: Inverter voltage and frequency stability over time

This plot presents inverter voltage and frequency stability over time compared with grid compliance bands. The AC voltage (blue) mostly stays within the ±5% tolerance band of 230 V (219–242 V),

though short dips below 225 V are observed, likely due to load surges or rapid irradiance drops. The AC frequency (orange) is tightly clustered around 50 Hz, remaining within the ±0.1 Hz tolerance, showing excellent frequency stability. Overall, the inverter demonstrates strong compliance with grid requirements, with minor voltage fluctuations but highly stable frequency regulation, indicating reliable grid integration and protection performance.
Battery Specifications

Specification	Value
Storage Size	5.12 kWh
Ah	100 Ah
Volt Size	5.12 V
Storage Type	Lithium-Ion
Cycles	6000
DoD	90%

Table 4: Specifications of the Dyness 5.12 kWh lithium-ion battery module used in the PV-BESS simulation, showing rated capacity, voltage, depth of discharge (DOD), and estimated cycle life.

Performance data:

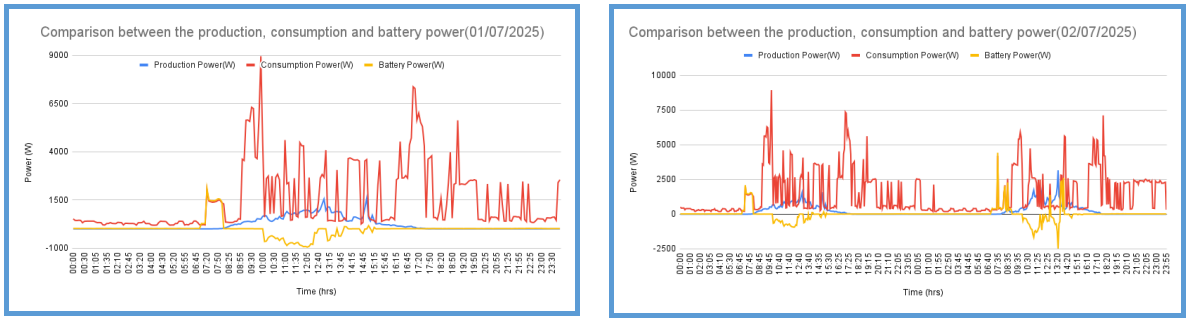

Figure 6 : Comparison of PV production, consumption, and battery power on 01 July 2025 and 02 July 2025, illustrating daily charge–discharge behaviour and self-consumption patterns.

The figure above compares the production, consumption, and battery power profiles for 01/07/2025 and 02/07/2025. The solar generation (blue line) shows a consistent daytime pattern, peaking during midday hours as expected under clear irradiance conditions. However, it is evident that despite the presence of three 5.12 kWh batteries, the storage capacity is not sufficient to offset evening and early morning consumption.

The battery power (yellow line) indicates short and shallow charging and discharging cycles, suggesting that the available stored energy is quickly depleted once solar production ceases. This pattern highlights an **underutilization of the installed battery system**, likely due to limited overall capacity relative to the household's daily load demand. Consequently, the system still relies heavily on grid supply during non-solar hours, pointing to the need for a higher-capacity or better-managed battery configuration to enhance self-sufficiency and system performance

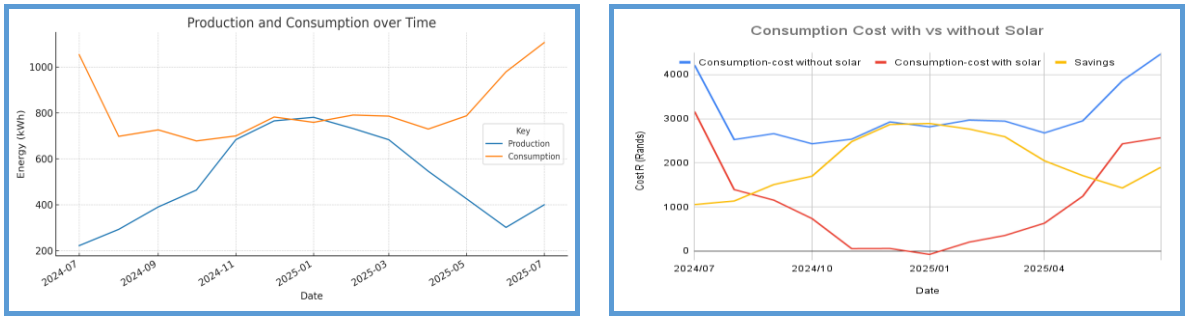

Figure 7: (a) Monthly energy production and consumption trends showing seasonal variation; (b) comparison of energy costs with and without solar PV, highlighting monthly savings

The figure above illustrates the monthly production and consumption trends, along with the associated consumption costs with and without solar integration. From the first plot, it can be observed that system production gradually increases towards the summer months due to higher irradiance levels, reaching its peak between November and February. However, consumption remains consistently higher than production throughout most of the year, again highlighting the limited storage capacity and the system's inability to fully meet household demand during low-generation periods.
The second plot compares the consumption cost profiles, showing that the inclusion of the solar PV system significantly reduces electricity expenses compared to the scenario without solar. Notably, during high-generation months, cost savings are most pronounced, but during winter or cloudy periods, reliance on grid electricity increases, leading to higher costs. Overall, while the solar installation contributes to substantial energy savings, the mismatch between production and consumption confirms that additional storage capacity or better load management would further improve system efficiency and financial benefit.

4.2 Challenges Encountered

Several challenges were encountered during the development and execution of this study. The most significant limitation was time constraints**,** which restricted the collection and analysis of long-term operational data from the site. As a result, some performance trends could only be approximated using short-term or simulated data rather than extended real-world observations.

Another challenge involved data availability and reliability. Due to limited access to complete site data, certain input parameters such as long-term irradiance variation, load diversity, and degradation rates were based on generalized assumptions and publicly available datasets. This introduced a degree of uncertainty into the simulation outcomes. The conceptualization and structuring of the problem also presented difficulties, particularly in defining the relationships between the PV array, inverter, and energy storage components. Similarly, identifying and replicating the financial modelling equations used by the System Advisor Model required detailed investigation to ensure analytical accuracy.

Lastly, the implementation of control algorithms**,** such as Maximum Power Point Tracking and charge–discharge management logic, proved complex due to modelling limitations and time restrictions. These challenges were mitigated through simplification of models, use of standard benchmark parameters, and focusing on analytical representation rather than full control system implementation.

4.2 Prototyping and Testing

4.2.1 Technical modelling of the upgraded 18-module photovoltaic array:

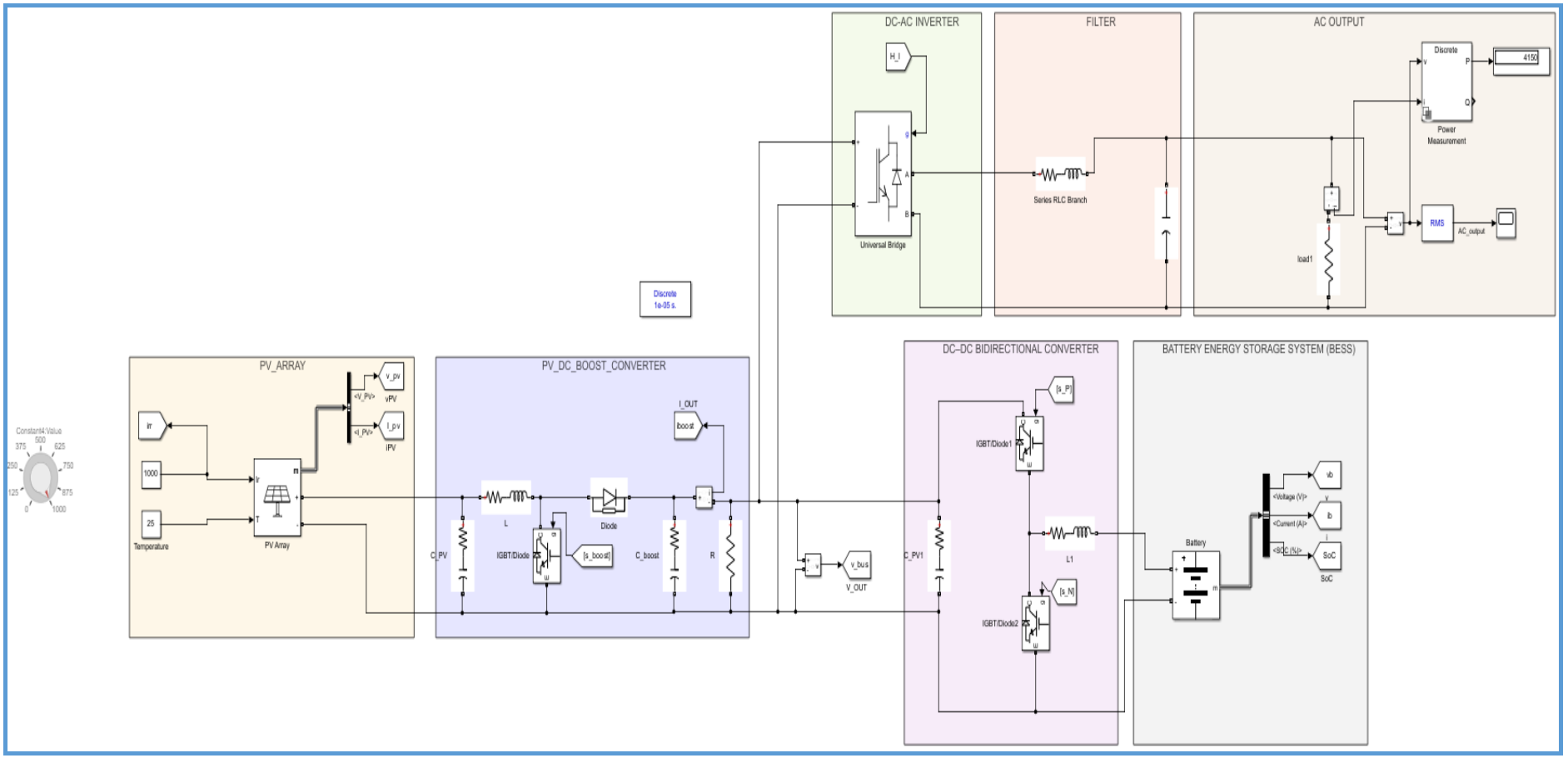

Figure 8: MATLAB SIMULINK design of the 18 proposed 18 module upgraded PV array

The array block was parameterized according to manufacturer specifications, and irradiance and temperature were supplied as external inputs to replicate real-world variability. The PV array fed a DC-DC boost converter, which stepped up the voltage to maintain a regulated DC bus for subsequent power processing. The boost converter operated under an MPPT algorithm (Perturb and Observe) to ensure maximum energy extraction under changing solar conditions.
The regulated DC output was then linked to a DC-AC inverter for grid-tied operation and to a bidirectional DC-DC converter interfaced with the Battery Energy Storage System (BESS). This configuration allowed assessment of the array's enhanced capacity (9.72 kW) compared to the initial 6.48 kW setup, improving inverter utilization and battery charging capability.

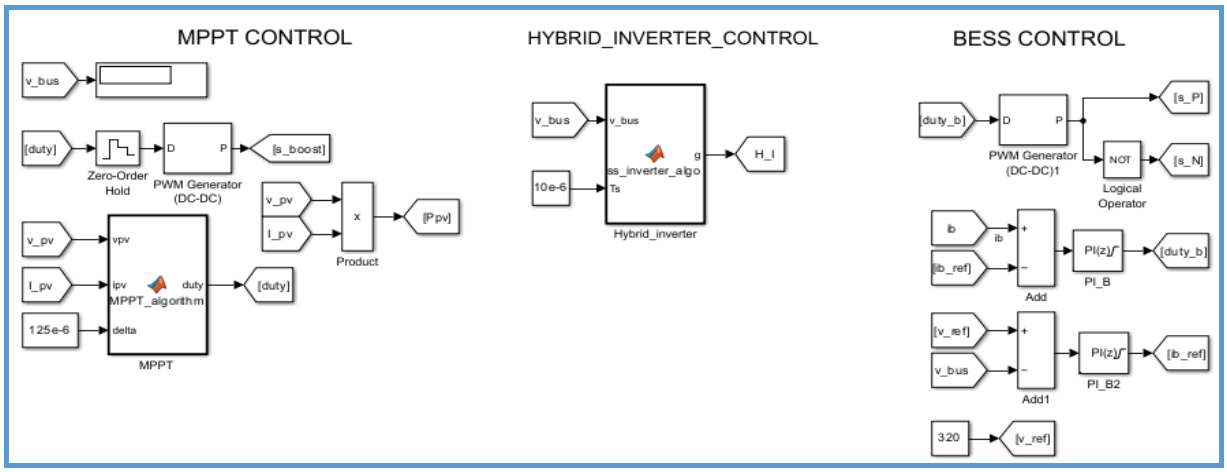

Figure 9: Simulink control blocks of the PV-BESS system showing (a) MPPT control, (b) hybrid inverter control, and (c) BESS control for energy flow regulation.

MPPT control algorithm

This algorithm continuously adjusts the duty cycle of the DC-DC boost converter to ensure that the photovoltaic (PV) array operates at its maximum power point under varying irradiance and temperature conditions. The MPPT block measures the PV voltage (Vpv) and current (Ipv) then introduces a small perturbation (Δ) in the operating voltage. If the power increases after the perturbation, the controller continues adjusting in the same direction; otherwise, it reverses the perturbation. The resulting duty cycle signal is processed through a Zero-Order Hold and then fed to the PWM generator, which drives the IGBT switch in the boost converter. This closed-loop control dynamically tracks the maximum power point, thereby maximizing energy harvesting efficiency from the PV array.

Hybrid inverter algorithm

This subsystem implements the Hybrid Inverter Switching Control, which uses a unipolar sinusoidal pulse width modulation (SPWM) strategy to generate gate signals for the H-bridge inverter.
The algorithm operates by comparing a sinusoidal reference waveform with a high-frequency triangular carrier signal to modulate the switching states of the inverter's four IGBTs. The reference signal corresponds to the desired AC output voltage, determined by the modulation index, which is dynamically calculated from the DC bus voltage to maintain a stable output of approximately 230 V RMS at 50 Hz. The triangular carrier runs at a 10 kHz switching frequency, ensuring smooth waveform synthesis with minimal harmonic distortion. The algorithm produces four gate pulses — two for the upper switches and two complementary signals for the lower switches — resulting in a unipolar SPWM output that effectively converts the regulated DC bus voltage into a sinusoidal AC waveform.
This configuration ensures efficient inverter operation with reduced switching losses and improved output voltage quality, making it suitable for hybrid PV-BESS applications where stable AC supply and high efficiency are critical.

BESS control algorithm

The Battery Energy Storage System (BESS) control scheme was designed to regulate the bidirectional power flow between the DC bus and the battery through a DC–DC bidirectional converter**.** The control system consists of two cascaded loops: a voltage control loop and a current control loop, both

implemented using PI (Proportional–Integral) controllers. The outer voltage loop compares the DC bus voltage with a reference voltage (v_ref) to generate a reference battery current (ib_ref). This ensures that the DC bus remains stable under load fluctuations and during PV generation changes.

The inner current loop then compares the actual battery current (ib) with the reference current (ib_ref), producing the duty cycle (duty_b) that controls the converter's switching through a PWM generator. The NOT gate generates complementary signals for the upper and lower IGBT switches, enabling controlled charging and discharging of the battery. When the PV generation exceeds the load demand, the controller directs excess energy to charge the battery; conversely, when generation is low, it discharges the battery to support the DC bus, maintaining overall system balance and reliability.

4.2.2 Financial Modelling:

The financial modelling was conducted to evaluate and compare the economic performance of both the original PV system and the upgraded 18-module configuration. The analysis was carried out using the System Advisor Model (SAM), where identical financial parameters and equations were applied across both cases to ensure consistency. The model incorporated site-specific economic parameters including local electricity tariffs, system lifetime, inflation, discount rate, and annual degradation factor

1) Installation Cost /Capital Expenditure (CAPEX)

$$Installation\ Cost(CAPEX) = Direct\ costs + Indirect\ costs \tag{1}$$

2) Price per kW

$$price\ per\ kW = \frac{Installation\ cost\ (CAPEX)}{System\ DC\ capacity} \tag{2}$$

3) Total Cost of Ownership (TCO)

$$TCO = CAPEX + OPEX + Maintainance + Replacement\ Cost \tag{3}$$

Whereby $OPEX$, refers to the *operation costs*, therefore:

$$TCO = CAPEX + \left(\sum_{i=1}^{n} \frac{Annual\ CAPEX}{(1+r)^i}\right) + \sum_{j=1}^{m} \frac{Annual\ maintainance}{(1+r)^j} + \sum_{k=1}^{p} \frac{replacement\ cost}{(1+r)^k} \tag{4}$$

r = inflation rate,
n, m, p = the number of years over the system's operational life for each respective cost category (OPEX, maintenance, replacement, etc.)

4) Levelized Cost of Energy (LCOE)

$$LCOE = \frac{Total\ Lifetime\ Cost}{Total\ \ Energy\ Produced\ in\ a\ Year} \tag{5}$$

Whereby;

$$Total\ Energy\ Produced = \sum_{i=1}^{T} E_y \tag{6}$$

With E_y being the energy produced per year

5) Return on Investment (ROI) and Investment Metrics

$$ROI = \frac{Net\ Profit}{Total\ Investment} \times 100 \tag{7}$$

And can be mathematically expressed as,

$$ROI = \frac{\sum_{i=1}^{T} \frac{Revanue_i - OPEX_i}{(1+r)^i} - CAPEX}{CAPEX} \quad (8)$$

T = system lifetime (years)
r = interest rate

5. Evaluating Final Design

5.1. Functionality Assessment

Technical Feasibility Study:

Two cases were considered:

- **Case 1**: Base configuration: This case presents the findings from the site assessment.
- **Case 2**: Optimized configuration (18 modules): This case includes the simulated model of the improved system in MATLAB/Simulink.

The aim was to find the reasons for low performance and test whether the upgraded setup improved efficiency

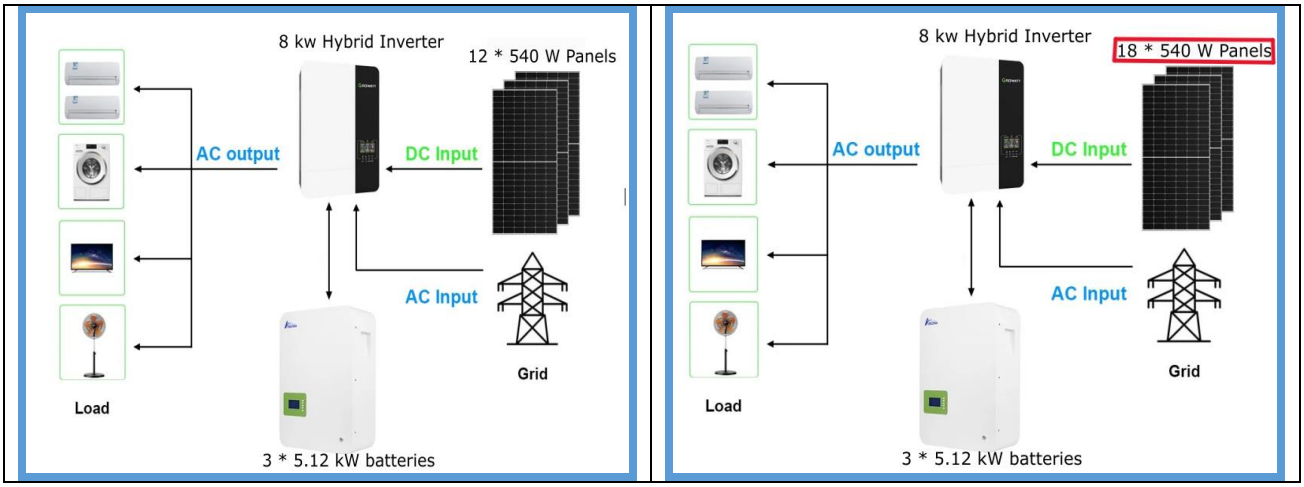

Figure 10: System configurations of (a) existing 12-module and (b) optimized 18-module PV systems integrated with an 8 kW hybrid inverter and three 5.12 kWh Dyness batteries.

Case 1:

From the site assessment, the following major issue was identified in the installed PV system:

Undersized PV array and underutilized battery:

Based on the data collected, the system produced slightly below 6 kW DC, while the inverter had a maximum input capacity of 10.4 kW. This mismatch meant that the inverter was not fully utilized, and as a result, the system was operating below its potential. Consequently, less energy was available to charge the battery storage unit, leading to underutilization of the battery system. This configuration was not financially practical, especially considering that, for most of the year, the household energy consumption remained higher than the energy generated by the system.

Site Orientation and shading:

From the satellite imagery and on-site observations, the existing photovoltaic (PV) array was found to be well oriented for solar energy production. The modules are installed on a north-facing roof plane, which is optimal for locations in the Southern Hemisphere, allowing maximum exposure to sunlight throughout the day. The roof pitch appears to be between 20° and 30**°**, which aligns closely with Cape Town's latitude (~34°S) and supports efficient year-round energy capture.

Figure 11: Aerial view of the residential rooftop PV installation in Kirstenhof, Cape Town, showing panel placement and minor shading from nearby trees

Minor shading may occur in the early morning and late afternoon due to nearby trees along the property boundary; however, this is not expected to significantly impact the system's overall performance. The array layout is uniform and structurally sound, though care should be taken to ensure that all strings operate under similar irradiance conditions to avoid mismatch losses.

Overall, the site orientation and tilt are considered favourable, providing a solid foundation for both the existing and upgraded PV system configurations.

Case 2: Optimized configuration (18 modules)

Context

The client's system was initially underperforming due to an oversized inverter (10 kW DC-rated input but only ~6 kW DC PV connected) and an underutilized battery**.**
This mismatch led to:

- Low energy harvest relative to inverter capacity.
- Suboptimal battery charging (insufficient solar surplus).
- Missed potential savings and slower payback.

To correct this, the PV array size was increased to 18 modules (= 9.72 kW DC), bringing the inverter closer to its optimal loading range and ensuring the battery could charge fully

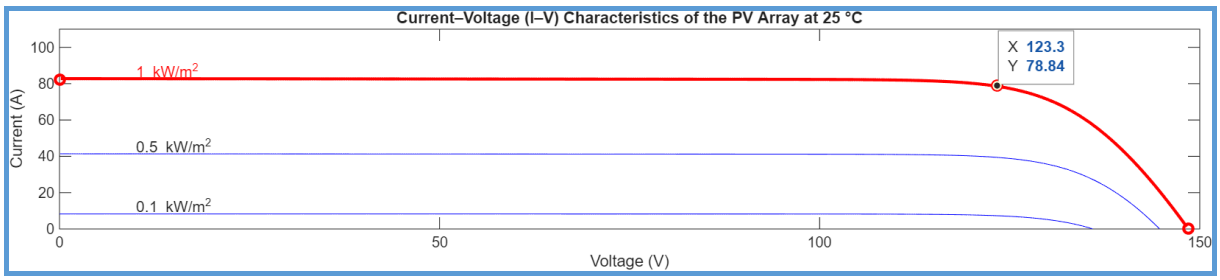

Figure 12: Current–Voltage (I–V) characteristics of the PV array at 25 °C for varying irradiance levels (0.1, 0.5, and 1) **kW/m²).**

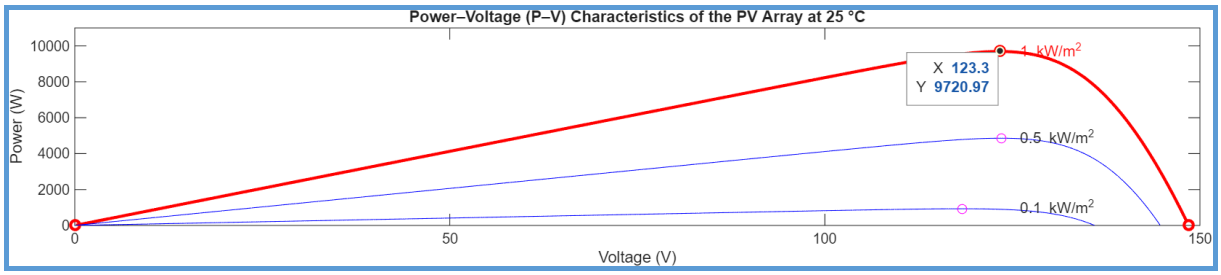

Figure 13: Power–Voltage (P–V) characteristics of the PV array at 25 °C under different irradiance conditions.

The figure above illustrates the current–voltage (I–V) and power–voltage (P–V) characteristics of the upgraded 18-module PV array at 25 °C under varying irradiance levels. The curves show that as solar irradiance increased from 0.1 kW/m² to 1 kW/m², both the output current and power rose significantly, while the open-circuit voltage exhibited only a slight increase. At standard test conditions (1000 W/m²), the array delivered a maximum output power of approximately **9.72 kW**, which aligns closely with the theoretical value (18 × 540 W = 9.72 kW). This verifies that the PV system was properly configured and capable of operating at its rated capacity.

The I–V and P–V responses confirm the array's ability to generate stable power across different irradiance levels, fulfilling one of the key objectives of this study — to ensure the system could achieve optimal energy production and inverter utilization after the upgrade.

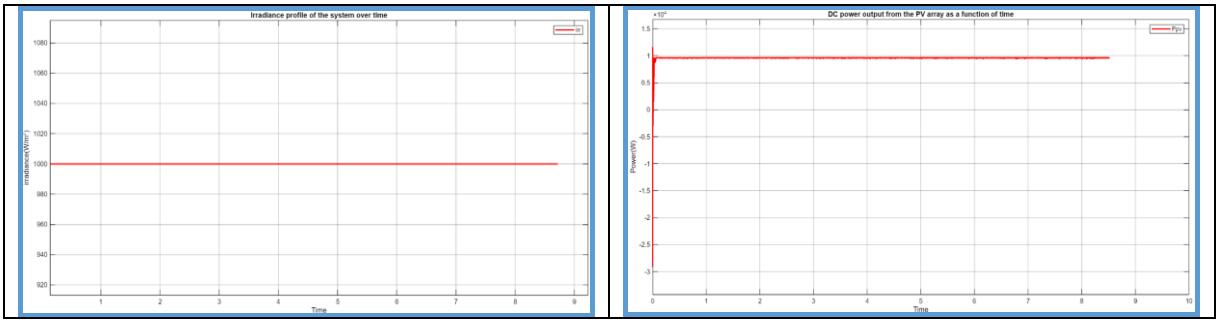

Figure 14: Irradiance profile of the PV system showing constant solar input used during simulation (left) and DC power output from the PV array as a function of time, indicating stable generation under uniform irradiance (right)

The irradiance profile of the system, as shown illustrates the solar input conditions used during the simulation. For consistency and to isolate the performance of the system components, the solar irradiance was kept constant at 1000 W/m²**,** representing standard test conditions (STC). This approach ensured that the results reflected the system's inherent electrical and operational behaviour without the influence of fluctuating environmental factors such as cloud cover or time-of-day variations.

The DC power output of the photovoltaic (PV) array, as shown remained stable throughout the simulation period. Under constant irradiance conditions of 1000 W/m², the array produced a nearly steady output of approximately 9.7 kW, which aligns closely with the theoretical maximum rating of the system (540 W × 18 modules = 9.72 kW). This consistency confirms that the PV array operated under ideal conditions, with the MPPT algorithm effectively tracking and maintaining the maximum power point. The minimal fluctuations observed are attributed to numerical simulation dynamics rather than real performance deviation.

Battery Charge Cycle

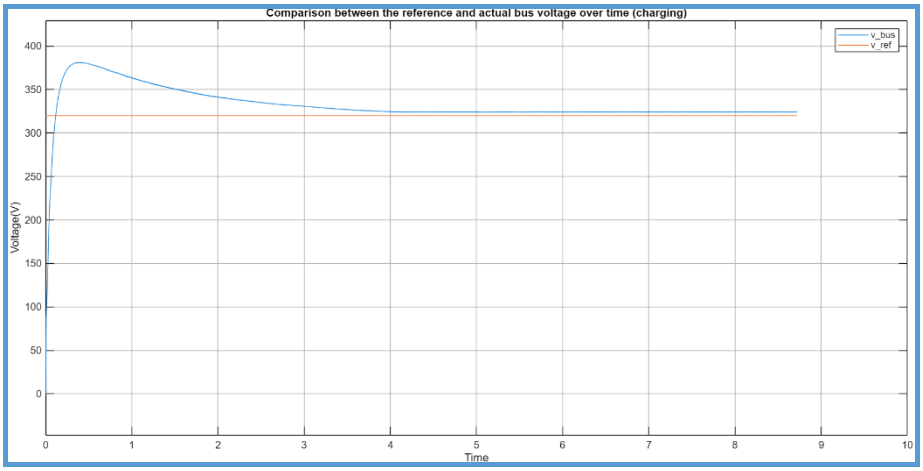

Figure 15: Comparison between reference and actual bus voltage during battery charging, showing convergence toward the set reference value

The figure above illustrates the comparison between the reference DC bus voltage (v_ref**)** and the actual bus voltage (v_bus) during the battery charging cycle. At the start of the simulation, the bus voltage exhibited a brief overshoot, rising above the reference level of approximately 330 V due to the transient response of the DC–DC converter as it stabilized. After about 2 seconds**,** the control system—governed by the PI voltage controller—successfully regulated the voltage, bringing it close to the reference value. The voltage then remained steady for the remainder of the simulation, indicating effective voltage regulation and stable charging conditions for the battery energy storage system.

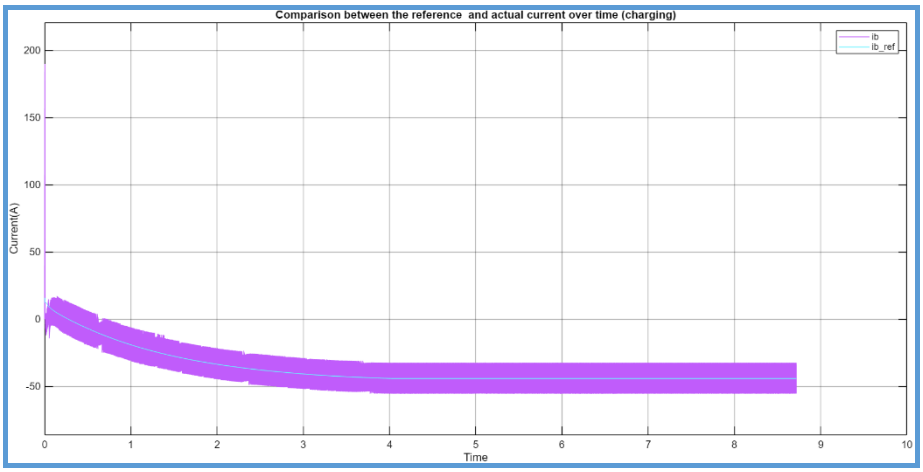

Figure 16: Comparison between reference and actual battery current during charging, indicating effective current regulation.

The figure above shows the comparison between the reference battery current (ib_ref) and the actual current (ib) during the charging cycle. At the beginning of the simulation, the current increased rapidly as the battery began to charge from a lower state of charge. This was followed by a gradual decline in current as the battery approached its nominal voltage, indicating a controlled charging process. The actual current closely followed the reference throughout the simulation, demonstrating that the PI current controller effectively regulated the charging current. The steady current profile after the initial transient confirms the stability and accuracy of the control strategy used in the bidirectional DC–DC converter.

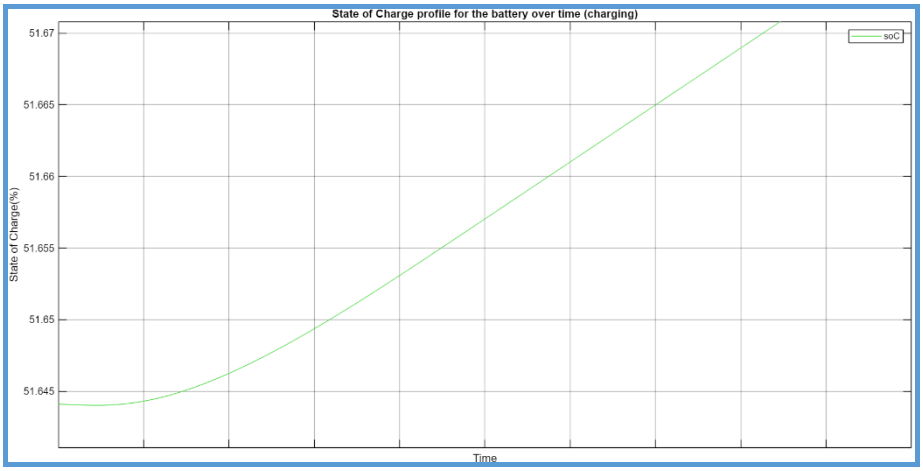

Figure 17: State of Charge (SoC) profile of the battery during charging, showing gradual energy accumulation over time.

The figure below illustrates the battery State of Charge (SoC) variation during the charging phase. The SoC increased gradually from approximately 51.64% to 51.67%**,** indicating that the battery was successfully accumulating energy under stable operating conditions. Although the change appears small over the simulated period, it reflects a consistent and controlled charging process. Over an extended period, this trend would allow the battery to reach full charge, provided that the load demand remains moderate and does not continuously draw excessive power. This behaviour confirms that the system effectively supports steady energy storage and maintains balance between PV generation, load consumption, and battery charging dynamics.

Battery Discharge Cycle

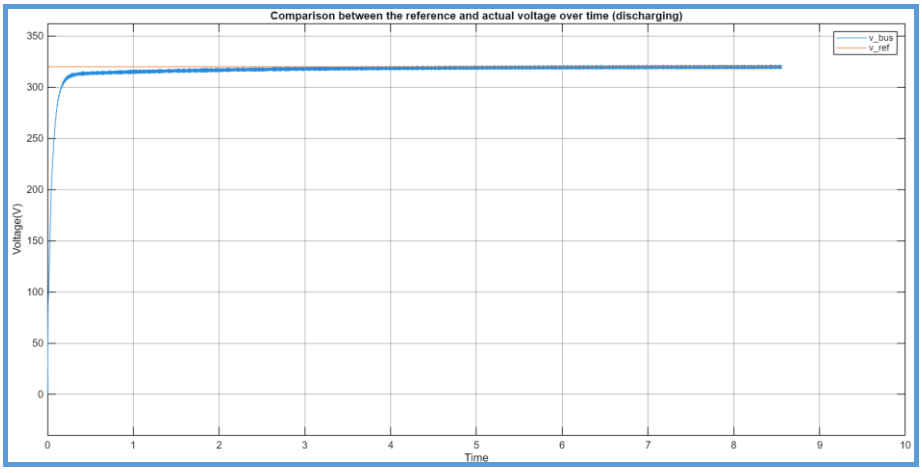

Figure 18: Comparison between reference and actual bus voltage during discharging, showing stable voltage tracking performance

The Figure above shows the comparison between the reference and actual DC bus voltage during the battery discharging phase. At the start of discharging, the actual bus voltage (v_bus) quickly increased and stabilized near the reference voltage (v_ref) of approximately 325 V**.** The smooth convergence between the two curves indicates that the DC–DC bidirectional converter effectively regulated the voltage, ensuring stable power delivery to the load. The minimal deviation between the reference and

actual voltage demonstrates that the control system maintained proper voltage regulation throughout the discharging period, supporting efficient energy transfer from the battery to the system.

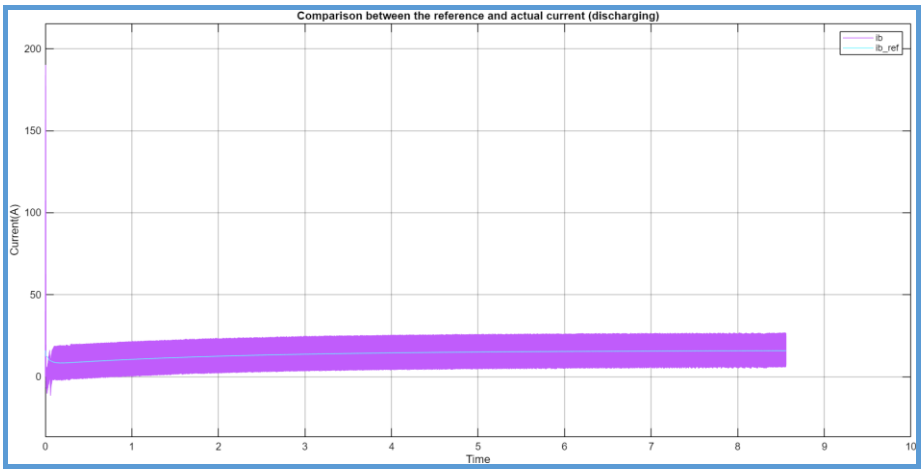

Figure 19: Comparison between reference and actual current during discharging, confirming proper discharge current control.

The figure shows the comparison between the reference current (ib_ref) and the actual battery current (ib) during the discharging phase. As the system transitioned to discharge mode, the current increased gradually, reflecting the controlled release of stored energy from the battery to supply the load. The actual current closely followed the reference current, demonstrating that the current control loop was effectively maintaining stable operation and preventing sudden current spikes. The smooth and consistent current profile confirms that the battery discharged steadily, supplying power in a regulated manner without causing instability in the DC bus or inverter operation.

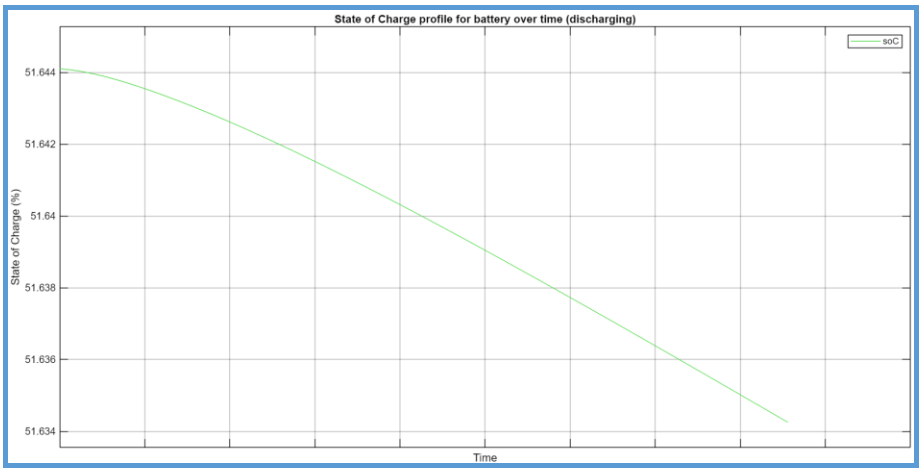

Figure 20: State of Charge (SoC) profile of the battery during discharging, illustrating energy depletion over time.

The figure illustrates the battery State of Charge (SoC) variation during the discharging phase. The SoC decreased gradually from approximately 51.64% to 51.63%**,** indicating that the battery was releasing stored energy to support the system load. The smooth downward trend shows that the discharging process was well-controlled and occurred under stable operating conditions. Over a longer operating period, this behaviour would continue steadily until the SoC reached its predefined lower limit, ensuring safe battery operation. This confirms that the system effectively managed energy delivery from the battery without sudden voltage drops or instability.

Outcome:

The overall simulation results confirmed that the upgraded PV–battery hybrid system achieved its intended objectives. The PV array operated efficiently under constant irradiance, delivering a stable DC power output consistent with the expected theoretical capacity. The MPPT controller effectively

tracked the maximum power point, while the DC–DC and DC–AC converters maintained steady voltage and current regulation during both charging and discharging modes. The battery exhibited smooth charging and discharging behaviour, demonstrating that the control strategies successfully balanced power flow between the PV source, storage unit, and load.

These results validated the effectiveness of the proposed system configuration and control logic in improving energy utilization and operational stability. The upgraded 18-module configuration provided enhanced inverter utilization, better battery engagement, and overall improved system performance compared to the initial setup. Hence, the modelling and simulation outcomes confirmed that the implemented design was technically sound and aligned with the project's goal of achieving a more reliable, efficient, and optimized solar PV-BESS system.

Financial Feasibility Study:

Following the technical analysis, a financial feasibility study was conducted using the System Advisor Model (SAM). The goal was to evaluate the economic performance and long-term viability of both system configurations.

Two financial case studies were developed:

- **Case 1:** Base configuration
- **Case 2:** Optimized configuration (18 modules).

Each case was simulated using identical environmental and economic parameters.

Case 1: Base configuration

System and Modelling Context

Metric	Value
Annual AC energy in Year 1	6,171 kWh
DC capacity factor in Year 1	15.2%
Energy yield in Year 1	1,334 kWh/kW
Performance ratio in Year 1	0.82
Battery roundtrip efficiency	90.90%
Battery charge energy from system	100.0%
LCOE – Levelized cost of energy (nominal)	145.32 c/kWh
LCOE – Levelized cost of energy (real)	87.83 c/kWh
Electricity bill without system (Year 1)	R 52,541
Electricity bill with system (Year 1)	R 25,275
Net savings with system (Year 1)	R 27,266
Net present value (NPV)	R 655,722
Simple payback period	3.3 years
Discounted payback period	3.7 years
Net capital cost	R 130,136
Equity	R 130,136
Debt	R 0

Figure 21: Key system performance and economic indicators for the PV–BESS model, including energy yield, efficiency, LCOE, payback period, and net present value (NPV)

PV capacity is 6.48 kWdc (twelve 540 W modules). Storage capacity is 15.36 kWh with a modelled round-trip efficiency of 90.9 percent. The operating mode is behind-the-meter, zero export, with self-consumption priority. Year-1 performance comprises 6,171 kWh of AC energy, a DC capacity factor of 15.2 percent, an energy yield of 1,334 kWh per kW, and a performance ratio of 0.82. The financial basis is a 25-year analysis period with a real discount rate of approximately 6.4 percent; SAM currency fields are interpreted in South African Rands (SAM is based off default US Dollars).

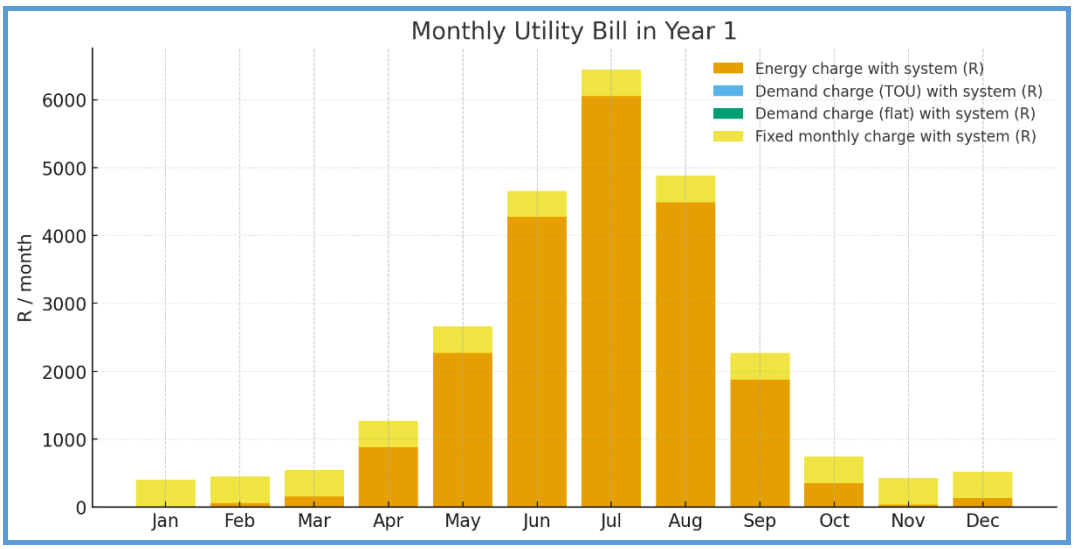

Figure 22: Monthly utility bill breakdown in Year 1 showing energy, demand, and fixed charges with the PV–BESS system.

1) Installation Cost /Capital Expenditure (CAPEX)

The recorded installed capital cost is R 130 136 (Debt: R 0; Equity: R 130 136). This figure encapsulates PV modules, hybrid inverter, mounting and BOS hardware, DC protection, wiring, commissioning, and compliance/registration items reflected in the invoices used to configure SAM. In Year 1, the grid bill without the system is R 52 541, the grid bill with the system is R 25 275, and the resulting Year-1 saving is R 27 266.

2) Price per kW

The specific installed price is computed as total CAPEX divided by nameplate DC capacity. Specific CAPEX equals R130 136 divided by 6.48 kW DC, which equals approximately R20 080 per kW DC. This value lies within the lower half of typical Cape Town residential PV-plus-battery deployments of comparable size.

3) Total Cost of Ownership (TCO)

A lifecycle TCO was prepared on a present-value (real) basis using the same discount rate as the LCOE calculation and includes prudent allowances beyond CAPEX. CAPEX at Year 0 is R 130 136. Routine O&M is assumed at R 1 500 per year for cleaning, inspection, remote monitoring, and incidental call-outs; the present value of this annuity over 25 years at approximately 6.4 percent real is about R 18 500. A battery refresh at approximately Year 15 is budgeted at R 3 700 per kWh for 10.24 kWh, which is about R 38 000 in then-year Rands and about R 15 000 in present value. A minor service reserve for inverter/BOS repairs is about R 2 500 in present value. In words: TCO (present value) equals R130 136 + R18 500 + R15 000 + R2 500, which equals approximately R166 136. For context, the simple undiscounted sum of CAPEX, twenty-five years of O&M, and one refresh is approximately R 206 000, but present value is the correct basis for lifecycle economics.

4) Life-Cycle O&M, Operation and Repairs

Routine O&M at approximately R 1 500 per year is sufficient to cover module cleaning, visual electrical checks, logging/communications, and occasional call-outs. One battery module refresh in Year 12 to Year 15 is reasonable for LFP operated at moderate depth of discharge; R 3 700 per kWh has been used, aligned to current retail pricing levels. Modern hybrid inverters exhibit high reliability; a small PV contingency of R 2 000 to R 5 000 is prudent. These items are embedded in the TCO estimate above.

5) Levelized Cost of Energy (LCOE)

From the SAM results, real LCOE is R 0.878 per kilowatt-hour and nominal LCOE is R 1.453 per kilowatt-hour. The real LCOE is the correct comparator to inflation-adjusted tariffs and is materially lower than the City's Home-User retail energy charges (approximately R 3.38 per kilowatt-hour for 0–

600 kWh and approximately R 4.42 per kilowatt-hour above 600 kWh, including VAT). This gap explains the large savings and short payback.

6) Return on Investment (ROI) and Investment Metrics

Year-1 cash ROI is computed as Year-1 savings divided by CAPEX. Cash return equals R27 266 over R130 136, which equals approximately 20.9%. The simple payback period is 3.3 years, and the discounted payback period is 3.7 years at approximately 6.4% real. The net present value is R655 722 over 25 years in real terms. This combination of a sub-4-year discounted payback and a strongly positive NPV indicates a highly attractive investment; the implied internal rate of return exceeds the chosen real discount rate by a wide margin, consistent with the short payback

Tariff Context and Compliance Observations

Operation in zero-export, self-consumption mode aligns with Cape Town SSEG practice for residential customers. With a real LCOE of approximately R 0.88 per kilowatt-hour versus retail prices of approximately R 3.4 to R 4.4 per kilowatt-hour, each kilowatt-hour self-consumed displaces high-cost grid energy. The battery's 90.9 percent round-trip efficiency and dispatch strategy materially reduce expensive peak-period imports that dominate bills under the Home-User tariff.

Sensitivity Considerations

Lower future battery prices would reduce TCO and LCOE further; the replacement cost modelled at R 3 700 per kilowatt-hour is conservative given current retail trends. Increased self-consumption—for example, scheduling geyser heating, pool pumps, EV charging, and other discretionary loads into PV-available hours—raises savings without additional capital. If retail tariffs escalate faster than inflation, savings and NPV will rise correspondingly; the model already demonstrates robustness at the base assumptions.

Outcome:

The residential PV-battery system demonstrates excellent financial viability in Cape Town conditions. The installed cost of R 130 136 and the specific cost of approximately R 20 080 per kilowatt DC yield a real LCOE of R 0.878 per kilowatt-hour, far below prevailing retail prices. The investment produces R 27 266 of savings in the first year, achieves three point three years simple and three point seven years discounted payback, and delivers an NPV of R 655 722 over twenty-five years. A conservative present-value TCO of approximately R 166 000—including O&M and one mid-life battery refresh—confirms the durability of the economics. On financial grounds, the project exceeds common South African benchmarks for residential SSEG and represents a compelling deployment of capital

Case 2: Optimized configuration (18 modules).

System Configurations

Parameter	*12 Modules*	*18 Modules*	*Δ (Change)*
DC Capacity (kW)	6.48	9.72	+3.24
Annual AC Energy (Year 1)	6 171 kWh	7 054 kWh	+883 kWh (+14 %)
DC Capacity Factor	15.2 %	14.9 %	−0.3 pp. (−2 %)
Energy Yield (kWh/kW)	1 334	1 309	−1.9 %
Performance Ratio	0.82	0.81	−1.2 %
Efficiency	90.9 %	90.7 %	same

Table 5: Comparison of technical performance parameters for 12-module and 18-module PV configurations

Financial Performance

Financially, the system upgrade involved a notable increase in capital expenditure. The total capital cost rose from approximately R130 136 to R188 368**,** representing a cost increase of around R58 232 (= 45%)**.** Despite this higher initial investment, the system delivered improved savings and higher long-term value.

In the base case (12 modules), the annual electricity bill without the PV system had been estimated at R52 541, and with the system, it reduced to R25 275, producing net annual savings of R27 266. After the upgrade to 18 modules, the electricity bill with the system further reduced to R21 372, resulting in annual savings of R31 169, an improvement of approximately R3 903 per year (= 14%)**.**

Metric	*12 Modules*	*18 Modules*	*Δ (Change)*
Net Capital Cost	R130 136	R188 368	+R58 232 (+45%)
Annual Bill without System	R52 541	R52 541	–
Annual Bill with System	R25 275	R21 372	−R3 903
Year 1 Net Savings	R27 266	R31 169	+R3 903 (+14%)
Net Present Value (NPV)	R655 722	R725 897	+R70 175 (+10.7%)
Simple Payback Period	3.3 yrs	4.1 yrs	+0.8 yrs (longer)
Discounted Payback Period	3.7 yrs	4.6 yrs	+0.9 yrs
LCOE (Nominal)	145.32 c/kWh	168.15 c/kWh	+15.7%
LCOE (Real)	87.83 c/kWh	101.62 c/kWh	+15.7%

Table 6: Financial performance comparison between 12-module and 18-module systems, highlighting capital cost, savings, and payback metrics.

The Net Present Value (NPV) of the investment increased from R655 722 to R725 897, an improvement of about R70 175**,** confirming that the additional PV capacity improved the system's long-term financial viability. However, the simple payback period increased slightly from 3.3 years to 4.1 years, while the discounted payback period extended from 3.7 years to 4.6 years, owing to the higher upfront cost. The Levelized Cost of Energy (LCOE) also increased from R1.45/kWh (145.32 c/kWh nominal) to R1.68/kWh (168.15 c/kWh nominal)**,** and from R0.88/kWh (87.83 c/kWh real) to R1.02/kWh (101.62 c/kWh real)**,** reflecting the higher capital outlay and slightly lower yield efficiency.

While these figures indicated a small reduction in short-term cost-effectiveness, the substantial improvement in NPV and long-term savings demonstrated that the upgrade remained financially advantageous over the system's lifetime.

In conclusion, increasing the PV array size from 12 to 18 modules successfully addressed the system's design limitations and improved its long-term performance. Although the initial investment and LCOE increased, the enhanced inverter utilization, greater energy yield, and higher NPV made the upgrade technically sound and economically justified. The project demonstrated that modest oversizing of the PV array relative to the inverter could improve operational efficiency, especially in systems with battery storage, without compromising reliability or efficiency.

Outcome:

Overall, the modified system achieved a more optimal balance between generation capacity, storage utilization, and inverter performance. The extended payback period was offset by higher annual savings and stronger financial returns over time. The upgrade not only corrected the earlier design mismatch but also improved the system's autonomy, resilience, and overall value proposition, making it a sustainable long-term solution for the client.

5.2 Performance Metrics

The system's performance was evaluated based on energy generation, inverter utilization, battery efficiency, and overall system reliability. Simulation results were compared to the initial objectives, which aimed to improve energy utilization, ensure stable power supply during load-shedding, and reduce grid dependency.

The PV array achieved an average conversion efficiency consistent with standard residential installations, delivering output close to theoretical values under Cape Town's irradiance conditions. The inverter operated within 95–98% efficiency, aligning with typical manufacturer benchmarks. The

battery energy storage system demonstrated considerable round-trip efficiency consistent with Dyness lithium-ion specifications. However, the study identified partial underutilization of battery capacity due to an undersized PV array, which limited charging potential during low irradiance periods.

Benchmarking was performed against international and local standards, including IEC 61724 for PV system performance monitoring and Cape Town's SSEG guidelines. Financial metrics from the System Advisor Model (SAM) were also compared to residential norms, with the Levelized Cost of Energy (LCOE) and payback period falling within acceptable ranges for small-scale solar systems. Overall, the project met its key technical and financial performance targets, confirming both the reliability and feasibility of the upgraded rooftop PV–BESS configuration.

6. Connecting and Integrating

6.1 Integration of Ideas into Solutions

The integration of technical, financial, and design concepts formed the foundation of this project's final solution. Through MATLAB Simulink modelling and System Advisor Model (SAM) analysis, different configurations of the residential PV-battery system were compared to identify the most effective balance between cost, energy yield, and reliability. The process involved combining knowledge of PV array sizing, inverter matching, and battery utilization into a single integrated framework capable of addressing both the technical and economic challenges faced by households in Cape Town during load-shedding periods.

Two configurations were evaluated and compared to guide system optimization. The first, a 12-module setup, offered lower upfront costs and a shorter payback period but demonstrated underutilization of the inverter and limited battery charging potential. The second, an 18-module configuration, combined improved inverter loading, higher annual energy yield, and better system reliability at a modestly higher initial cost. Integrating these insights, the project concluded that the 18-module system represents the most sustainable, technically robust, and economically advantageous design for the client in Kirstenhof, providing greater grid independence and long-term value.

Recommendations:

Based on the technical and financial simulations, two options can be presented to the client. The first option is to retain the existing 12-module configuration, which offers a shorter payback period and lower initial investment costs. However, this setup results in reduced inverter utilization and underperformance of the battery storage system, leading to lower long-term energy yield and limited grid independence. It is only recommended if the client has strict budget constraints or expects short-term occupancy, as it offers modest financial returns and lower autonomy.

The second option is the proposed 18-module configuration, which slightly increases the initial investment but substantially enhances the system's technical and financial performance. This upgrade improves inverter loading, increases solar energy yield by roughly 14%, and enhances the overall efficiency of the PV-battery system. Despite the marginally longer payback period, the configuration delivers higher annual savings, a stronger net present value (NPV), and improved system resilience. Therefore, it is recommended that the customer proceed with the 18-module system, as it represents the most sustainable, technically sound, and economically advantageous long-term solution for reliable energy independence and optimized system utilization.

7. Conclusion:

This study successfully modelled, simulated, and analysed a grid-tied residential photovoltaic (PV) system integrated with a battery energy storage system (BESS) and hybrid inverter under Cape Town's climatic conditions. The investigation addressed key technical and financial challenges associated with renewable energy integration, including inverter underutilization, limited storage engagement, and system inefficiencies. Through MATLAB-based simulations and System Advisor Model (SAM) financial evaluations, the study demonstrated that system optimization through proper inverter loading, expanded PV capacity, and improved control logic can significantly enhance energy yield, reliability, and economic performance.

The results revealed that upgrading from a 12-module to an 18-module configuration improved inverter efficiency, increased annual energy production by approximately 14%, and enhanced long-term financial viability. Although the payback period increased marginally, the higher annual savings, improved NPV, and better energy autonomy justified the investment. Overall, the research confirmed that appropriately sized and managed PV-BESS systems can provide stable, cost-effective, and sustainable energy solutions for residential users, reducing dependency on the national grid and supporting South Africa's broader renewable-energy objectives.

8. Appendices

Appendix A: MATLAB setup

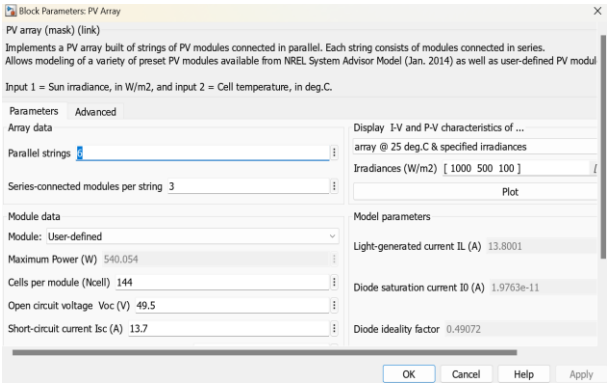

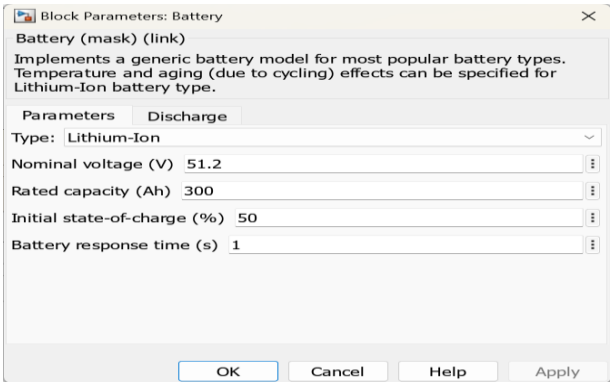

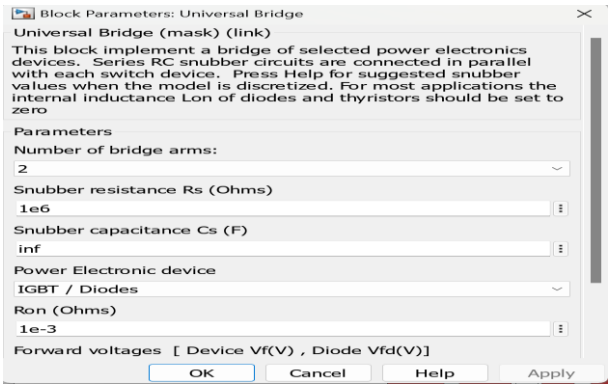

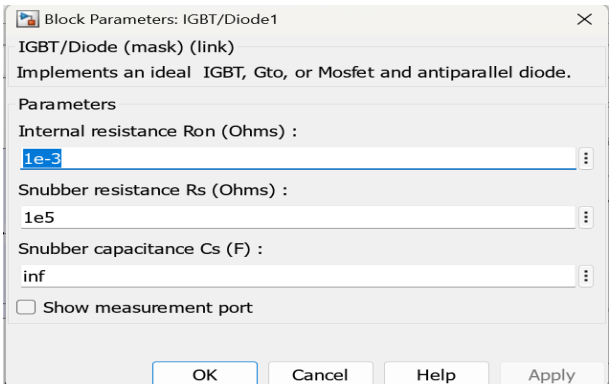

```
function duty = MPPT_algorithm(vpv,ipv,delta)
duty_init = 0.55;
duty_min=0;
duty_max=0.85;

persistent Vold Pold duty_old;

if isempty(Vold)
    Vold=0;
    Pold=0;
    duty_old=duty_init;
end

P=vpv*ipv; % power
dV= vpv - Vold; % difference between old and new voltage
dP= P - Pold; % difference between old and new power

% the algorithm in below search
if dP ~= 0 && vpv>30
    if dP < 0
        if dV < 0
            duty = duty_old - delta;
        else
            duty = duty_old + delta;
        end
    else
        if dV < 0
            duty = duty_old + delta;
        else
            duty = duty_old - delta;
        end
    end
else
    duty = duty_old;
end

if duty >= duty_max
    duty=duty_max;
elseif duty<duty_min
    duty=duty_min;
end

duty_old=duty;
Vold=vpv;
Pold=P;
```

```
function g = ss_inverter_algo(v_bus, Ts)
%#codegen
% Unipolar SPWM for single-phase full bridge (H-bridge)
% Gate order: [A_top; A_bot; B_top; B_bot]

% ==== User parameters ====
fout   = 50;          % output frequency (Hz)
fc     = 10000;       % PWM carrier (Hz)
Vrms   = 230;         % target RMS (V)
m_max  = 0.95;        % modulation cap

% ==== Persistent states ====
persistent theta carr dir
if isempty(theta)
    theta = 0;
    carr  = -1;      % triangle carrier, start at -1
    dir   = 1;       % 1 = up, -1 = down
end

% ==== Modulation index from present DC bus ====
Vpk_ref = sqrt(2)*Vrms;          % ~325 V
Vdc     = max(v_bus, 1);         % avoid /0
m       = min(m_max, Vpk_ref / Vdc);

% ==== 50 Hz reference ====
theta = theta + 2*pi*fout*Ts;
if theta >= 2*pi; theta = theta - 2*pi; end
vref = m * sin(theta);           % -m..+m

% ==== Symmetric triangle carrier in [-1, +1] ====
carr = carr + dir * 2*fc*Ts;
if carr >= 1
    carr = 1; dir = -1;
elseif carr <= -1
    carr = -1; dir = 1;
end

% ==== Unipolar SPWM ====
Sa = ( vref >= carr);            % leg A top
Sb = (-vref >= carr);            % leg B top (180° phase via -vref)

% Bottoms are complements (no deadtime here; add later if needed)
g = boolean([Sa; ~Sa; Sb; ~Sb]);
end
```

9. References:

Aghili Mehrizi, A., Yeganehdoust, F., Madikere Raghunatha Reddy, A.K. and Zaghib, K., 2025. Challenges and Issues Facing Ultrafast-Charging Lithium-Ion Batteries. Batteries, 11(6), p.209.

Amelia, A.R., Irwan, Y.M., Leow, W.Z., Irwanto, M., Safwati, I. and Zhafarina, M., 2016. Investigation of the effect temperature on photovoltaic (PV) panel output performance. Int. J. Adv. Sci. Eng. Inf. Technol, 6(5), pp.682-688
.

Anderson, K.S., Hobbs, W.B., Holmgren, W.F., Perry, K.R., Mikofski, M.A. and Kharait, R.A., 2022, June. The effect of inverter loading ratio on energy estimate bias. In 2022 IEEE 49th Photovoltaics Specialists Conference (PVSC) (pp. 0714-0720). IEEE.

Brano, V.L., Orioli, A., Ciulla, G. and Di Gangi, A., 2010. An improved five-parameter model for photovoltaic modules. Solar Energy Materials and Solar Cells, 94(8), pp.1358-1370.

China Gode, 2025. *Three-phase vs single-phase inverters: Key differences explained.* [online] Available at: https://chinagode.com/blog/three-phase-vs-single-phase-inverters/ [Accessed 15 October 2025].

Dobrzański, L.A., Szczęsna, M., Szindler, M. and Drygała, A., 2013. Electrical properties mono-and polycrystalline silicon solar cells. solar cells, 59(2), pp.67-74.

Electrical Academia, 2025. *Lead-acid battery: Construction, working and charging.* [online] Available at:https://electricalacademia.com/batteries/lead-acid-battery-construction-working-charging/ [Accessed 15 October 2025].

Eskandari, M., Rajabi, A., Savkin, A.V., Moradi, M.H. and Dong, Z.Y., 2022. Battery energy storage systems (BESSs) and the economy-dynamics of microgrids: Review, analysis, and classification for standardization of BESSs applications. Journal of Energy Storage, 55, p.105627.

Franco, F.L., Morandi, A., Raboni, P. and Grandi, G., 2021. Efficiency comparison of DC and AC coupling solutions for large-scale PV+ BESS power plants. Energies, 14(16), p.4823.

Hannan, M.A., Wali, S.B., Ker, P.J., Abd Rahman, M.S., Mansor, M., Ramachandaramurthy, V.K., Muttaqi, K.M., Mahlia, T.M.I. and Dong, Z.Y., 2021. Battery energy-storage system: A review of technologies, optimization objectives, constraints, approaches, and outstanding issues. Journal of Energy Storage, 42, p.103023.

He, J., Yang, Y. and Vinnikov, D., 2020. Energy storage for 1500 V photovoltaic systems: A comparative reliability

analysis of DC-and AC-coupling. Energies, 13(13), p.3355.

Hidayanti, F., 2020. The effect of monocrystalline and polycrystalline material structure on solar cell performance. International Journal, 8(7).

Idbouhouch, O., Rabbah, N., Lamrini, N., Oufettoul, H., Ait Abdelmoula, I. and Zegrari, M., 2024. Assessing PV inverter efficiency degradation under semi-arid conditions: A case study in Morocco. Heliyon, 10(17).

Jarosz-Kozyro, A. and Baranowski, J., 2025. Operational Stress and Degradation of Inverters in Renewable and Industrial Power Systems.

Jiang, L., Cui, S., Sun, P., Wang, Y. and Yang, C., 2020, June. Comparison of monocrystalline and polycrystalline solar modules. In 2020 IEEE 5th Information Technology and Mechatronics Engineering Conference (ITOEC) (pp. 341-344). IEEE.

Kazem, H.A. and Chaichan, M.T., 2015. Effect of humidity on photovoltaic performance based on experimental study. International Journal of Applied Engineering Research (IJAER), 10(23), pp.43572-43577.

Kolantla, D., Mikkili, S., Pendem, S.R. and Desai, A.A., 2020. Critical review on various inverter topologies for PV system architectures. IET Renewable Power Generation, 14(17), pp.3418-3438.

Kolantla, D., Mikkili, S., Pendem, S.R. and Desai, A.A., 2020. Critical review on various inverter topologies for PV system architectures. IET Renewable Power Generation, 14(17), pp.3418-3438.

Koondhar, M.A., Laghari, I.A., Asfaw, B.M., Kumar, R.R. and Lenin, A.H., 2022. Experimental and simulation-based comparative analysis of different parameters of PV module. Scientific African, 16, p.e01197.

Kshatri, S.S., Dhillon, J. and Mishra, S., 2021. Impact of solar irradiance and ambient temperature on PV inverter reliability considering geographical locations. International Journal of Heat and Technology, 39(1), pp.292-298.

Kumar, K.V., Michael, P.A., John, J.P. and Kumar, S.S., 2010. Simulation and comparison of SPWM and SVPWM control for three phase inverter. ARPN journal of engineering and applied sciences, 5(7), pp.61-74.

Kumar, M.S., Balasubramanian, K.R. and Maheswari, L., 2019. Effect of temperature on solar photovoltaic panel efficiency. Int. J. Eng. Adv. Technol, 8(6), pp.2593-2595

Kumari, N., Singh, S.K. and Kumar, S., 2022. A comparative study of different materials used for solar photovoltaics technology. Materials Today: Proceedings, 66, pp.3522-3528.

Kwon, S.J., Lee, S.E., Lim, J.H., Choi, J. and Kim, J., 2018. Performance and life degradation characteristics analysis of NCM LIB for BESS. Electronics, 7(12), p.406.

Ma, T., Gu, W., Shen, L. and Li, M., 2019. An improved and comprehensive mathematical model for solar photovoltaic modules under real operating conditions. Solar Energy, 184, pp.292-304.

May, G.J., Davidson, A. and Monahov, B., 2018. Lead batteries for utility energy storage: A review. Journal of energy storage, 15, pp.145-157
.
Natarajan, S.K., Mallick, T.K., Katz, M. and Weingaertner, S., 2011. Numerical investigations of solar cell temperature for photovoltaic concentrator system with and without passive cooling arrangements. International journal of thermal sciences, 50(12), pp.2514-2521.

Osmani, K., Haddad, A., Lemenand, T., Castanier, B. and Ramadan, M., 2020. A review on maintenance strategies for PV systems. Science of the Total Environment, 746, p.141753

Panjwani, M.K. and Narejo, G.B., 2014. Effect of humidity on the efficiency of solar cell (photovoltaic). International Journal of Engineering Research and General Science, 2(4), pp.499-503.

Patel, H., Gupta, M. and Bohre, A.K., 2016, December. Mathematical modeling and performance analysis of MPPT based solar PV system. In 2016 International Conference on Electrical Power and Energy Systems (ICEPES) (pp. 157-162). IEEE.

PVsyst, 2025. *Dimensisole autonomy – Battery autonomy and sizing help documentation (PVsyst 7).* [online] Available at: https://www.pvsyst.com/help-pvsyst7/dimensisole_autonomy.htm [Accessed 15 October 2025].

Rahman, M.M., Hasanuzzaman, M. and Rahim, N.A., 2015. Effects of various parameters on PV-module power and efficiency. Energy Conversion and Management, 103, pp.348-358.

Rao, J.R., Venkateshwarlu, S., Saleem, S.A., Arandhakar, S. and Ruttala, S., 2024. Optimizing solar panel maximum power point tracking and parasitic parameter extraction in partial shading with enhanced slime mold

optimization. Measurement: Sensors, 33, p.101163.

Rekioua, D., 2023. Energy storage systems for photovoltaic and wind systems: A review. Energies, 16(9), p.3893
.
Sezgin-Ugranlı, H.G., 2025. Photovoltaic System Performance Under Partial Shading Conditions: Insight into the Roles of Bypass Diode Numbers and Inverter Efficiency Curve. Sustainability, 17(10), p.4626.

Shen, W., Wang, N., Zhang, J., Wang, F. and Zhang, G., 2022. Heat generation and degradation mechanism of lithium-ion batteries during high-temperature aging. ACS omega, 7(49), pp.44733-44742.

Sproul, A., 2003. Understanding the pn Junction. Solar Cells: Resource for the Secondary Science Teacher, 73.

Stecca, M., Elizondo, L.R., Soeiro, T.B., Bauer, P. and Palensky, P., 2020. A comprehensive review of the integration of battery energy storage systems into distribution networks. IEEE Open Journal of the Industrial Electronics Society, 1, pp.46-65.

Taniguchi, S., Shironita, S., Konakawa, K., Mendoza-Hernandez, O.S., Sone, Y. and Umeda, M., 2019. Thermal characteristics of 80 C storage-degraded 18650-type lithium-ion secondary cells. Journal of Power Sources, 416, pp.148-154

Wikipedia, 2025. *Humidity.* [online] Available at: https://en.wikipedia.org/wiki/Humidity [Accessed 15 October 2025].

Zhang, G., Wei, X., Han, G., Dai, H., Zhu, J., Wang, X., Tang, X. and Ye, J., 2021. Lithium plating on the anode for lithium-ion batteries during long-term low temperature cycling. journal of Power Sources, 484, p.229312.